Environment International 191 (2024) 108950

Contents lists available at ScienceDirect

Environment International

journal homepage: www.elsevier.com/locate/envint

Full length article

Do greenspaces really reduce heat health impacts? Evidence for different vegetation types and distance-based greenspace exposure

Jinglu Song [a,*], Antonio Gasparrini [b], Di Wei [c,d,e], Yi Lu [c], Kejia Hu [f], Thomas B. Fischer [g,h], Mark Nieuwenhuijsen [i,j,k]

[a] Department of Urban Planning and Design, Xi'an Jiaotong-Liverpool University, Suzhou 215123, China
[b] Department of Public Health, Environment and Society, London School of Hygiene and Tropical Medicine, 15-17 Tavistock Place, London WC1H 9SH, UK
[c] Department of Architecture and Civil Engineering, City University of Hong Kong, Hong Kong, China
[d] School of Architecture and Urban Planning, Huazhong University of Science and Technology, Wuhan, China
[e] Hubei Engineering and Technology Research Center of Urbanization, Wuhan, China
[f] Institute of Big Data in Health Science, School of Public Health, Zhejiang University, Zijingang Campus, Hangzhou 310058, China
[g] Environmental Assessment and Management Research Centre, School of Environmental Sciences, University of Liverpool, Liverpool, UK
[h] Research Unit for Environmental Sciences and Management, Faculty of Natural and Agricultural Sciences, North West University, Potchefstroom, South Africa
[i] Barcelona Institute for Global Health (ISGlobal), Doctor Aiguader 88, Barcelona 08003, Spain
[j] Universitat Pompeu Fabra (UPF), Doctor Aiguader 88, Barcelona 08003, Spain
[k] CIBER Epidemiología y Salud Pública (CIBERESP), Melchor Fernández Almagro, 3-5, Madrid 28029, Spain

ARTICLE INFO

Keywords:
Extreme heat
Mortality risk
Greenspaces
Forest
Effect modifications

ABSTRACT

Background: While vegetation type, population density and proximity to greenspaces have been linked to human health, what type and location of greenspace matter most have remained unclear. In this context, there are question marks over investment-style metrics.
Objectives: This paper aims at establishing what vegetation type may matter most in modifying heat-mortality associations, and what the optimal buffer distances of total and specific types of greenspace exposure associated with reduced heat-related mortality risks are.
Methods: We conducted small-area analyses using daily mortality data for 286 Territory Planning Units (TPUs) across Hong Kong and 1 × 1 km gridded air temperature data for the summer months (2005–2018). Using a case time series design, we examined effect modifications of total and specific types of greenspaces, as well as population-weighted exposure at varying buffer distances (200–4000 m). We tested the significance of effect modifications by comparing relative risks (RRs) between the lowest and highest quartiles of each greenspace exposure metric; and explored the strength of effect modifications by calculating the ratio of RRs.
Results: Forests, unlike grasslands, showed significant effect modifications on heat-mortality associations, with RRs rising from 0.98 (95 %CI: 0.92,1.05) to 1.06 (1.03, 1.10) for the highest to lowest quartiles (p-value = 0.037) The optimal distances associated with the most apparent effects were around 1 km for population-weighted exposure, with the ratio of RRs being 1.424 (1.038,1.954) for NDVI, 1.191 (1.004,1.413) for total greenspace, and 1.227 (1.024,1.470) for forests. A marked difference was observed in terms of the paired area-level and optimal distance-based exposure to total greenspace and forests under extreme heat (p-values < 0.05).
Discussion: Our findings suggest that greenspace, particularly nearby forests, may significantly mitigate heat-related mortality risks.

1. Introduction

Due to global climate change, extreme heat events are becoming more frequent, intense, and longer in duration, leading to numerous impacts on the urban environment and population health (Intergovernmental Panel On Climate Change (IPCC), 2023). Heat-related mortality and morbidity are among the most direct and serious consequences of extreme heat. This has spurred action to combat heat

* Corresponding author at: Department of Urban Planning and Design, Xi'an Jiaotong-Liverpool University, 111 Renai Road, Suzhou 215123, China.
E-mail addresses: Jinglu.Song@xjtlu.edu.cn (J. Song), Antonio.Gasparrini@lshtm.ac.uk (A. Gasparrini), diwei3-c@my.cityu.edu.hk (D. Wei), yilu24@cityu.edu.hk (Y. Lu), kejiahu@zju.edu.cn (K. Hu), fischer@liverpool.ac.uk (T.B. Fischer), mark.nieuwenhuijsen@isglobal.org (M. Nieuwenhuijsen).

https://doi.org/10.1016/j.envint.2024.108950
Received 17 April 2024; Received in revised form 17 July 2024; Accepted 12 August 2024
Available online 13 August 2024

extremes in cities (Gasparrini et al., 2015, 2017; J. Wang et al., 2024). Nature-based solutions, such as urban forests, parks, street trees, lawns, shrubs, and gardens, collectively known as 'greenspace' (Panno et al., 2017; Swanwick et al., 2003), have shown great potential for mitigating climate-driven extreme events, contributing to adaptation and resilience (Kabisch et al., 2016; Zhao et al., 2022), and fostering human health and well-being in the context of urban settlements (Kabisch et al., 2017).

While there is now a relatively well-established evidence base for the potential of greenspaces to reduce heat-related mortality risks globally and regionally (Choi et al., 2022; Sera et al., 2019), protective effects remain inconclusive in studies at the local scale. While some intra-city studies suggest that living in greener areas has the potential to decrease health and death risks related to heat (Burkart et al., 2016; Harlan et al., 2013), some have also reported an absence of decreased heat mortality risk connected with residential greenspace (Gronlund et al., 2016; Madrigano et al., 2013; Xu et al., 2013). This variability is likely dependent on the availability of high-resolution data and the designs of statistical and computational methods (Gasparrini et al., 2022). While past studies that mainly relied on relevant data aggregated at a broader spatial scale may have overlooked the spatial contrasts of mortality risk and potential modifiers across fine-scale units (Choi et al., 2022; Sera et al., 2019), small-area analyses often have low statistical power (Murage et al., 2020; Son et al., 2016; Song et al., 2022). Importantly, although urban greening has a long history in some cities, its connection to heat mitigation strategies is not always clear. As the latter are proposed to be most effective when devised locally (Madrigano et al., 2015), understanding the exact effect of greenspace across fine-scale units is crucial for being able to provide a bridge between the two (Kabisch et al., 2016).

Even though urban greening is suggested to be a promising strategy to limit the negative health impacts of extreme heat, much remains to be learned about how to best promote and implement it (Hondula et al., 2018). Reviews of existing epidemiological studies generally conclude that simply by greening cities can the impacts of heat on health be mitigated (Schinasi et al., 2018; Son et al., 2019). However, city planners, politicians, and others involved in urban greening often require hard evidence demonstrating the health benefits of greenspace according to specific pathways (Markevych et al., 2017; Nieuwenhuijsen, 2018) and actionable information like investment-style metrics (Hondula et al., 2018; Iungman et al., 2023).

In terms of the existing professional literature, to date most authors have focused on an assessment solely of a single and simple measure of greenspace, such as the normalized difference vegetation index (NDVI) (Burkart et al., 2016; Madrigano et al., 2013; Son et al., 2016; Song et al., 2022; Zhang et al., 2021) or the proportion of greenspace (Gronlund et al., 2016; Pascal et al., 2021; Xu et al., 2013; Zanobetti et al., 2013). Though effective at assessing the overall level of greenspace in an area, these measures alone cannot capture the full spectrum of greenspace and do not take into account other factors that may influence heat-related health risks (Choi et al., 2022; Wu et al., 2018). Earlier research suggests that vegetation type, population density, and distance to greenspaces significantly impact public health (Ekkel & De Vries, 2017). However, their exact effects are unclear and appear to be dependent on specific pathways (i.e., heat mitigation) (Markevych et al., 2017). For example, as different vegetation types differ in their abilities to moderate temperatures (i.e., trees versus grass) (Bowler et al., 2010), the associated potential for heat mitigation will likely differ. However, what is currently poorly understood is how and to what extent different types of vegetation mitigate heat impacts on public health. In addition, a few studies have considered using population-weighted greenspace exposure (Heo et al., 2021) or calculating the average NDVI or percent tree cover within a specific buffer size around local residents (Madrigano et al., 2015; Pereira Barboza et al., 2023; Xu et al., 2013) to assess greenspace exposure more accurately. A recent study has also shown that street greenery may have higher health benefits against heat (Song et al., 2023). The more apparent effect modification is probably because street greenery could better represent the daily exposure to the accessible and proximate greenspace of local residents. However, it is still being established how proximate greenspace, or more specifically, what buffer size best represents the pathway linking greenspaces to heat health risk reduction and how exactly it works when considering population distribution in particular. These missing links weaken the potential for evidence to have an impact on decision-makers and on the creation of greenspace policies that will positively benefit health.

This paper reports on effect modifications of greenspace exposure on heat-mortality associations across the smallest planning units (i.e., Territory Planning Unit, TPU) in Hong Kong, using high-resolution data and case time series design. The authors aimed at extending existing knowledge by examining what vegetation types matter most in modifying heat-mortality associations, and what the optimal buffer distances of total and specific types of greenspace exposure associated with reduced heat-related mortality risks are.

2. Material and methods

2.1. Study design

We linked daily death records for 286 TPUs in Hong Kong during the summer months from June to October for the period 2005–2018 to TPU-specific daily temperatures derived from a 1 × 1 km gridded air temperature dataset. An extended case time series (CTS) model was then fitted in order to explore the effect modifications of area-level exposure to total and specific types of greenspace on heat-mortality associations. To identify optimal buffer distances, the population-weighted greenspace exposure and the associated increase in heat mortality risks were calculated within various buffer distances from residential areas (considering population distributions). In addition, the effect modifications of two sets of greenspace exposure metrics were compared by investigating the differences between the greenspace at the area level and exposed persons within the optimal buffer distance.

2.2. Data and exposure assessment

2.2.1. Daily mortality, weather and air pollution data

Individual mortality data were obtained from the Census and Statistics Department of Hong Kong from 2005 to 2018 for the months June to October. These anonymous records include information on date and underlying cause of death, and place of residence (in 3-digit TPU code). The cause of death was defined based on the Tenth Revision of the International Statistical Classification of Diseases, Injuries and Causes of Death (ICD-10). To retain a sufficient number of cases and to maximize the statistical power of analysis, the present study did not conduct further stratification by cause of death and include all-cause mortality that covers all known deaths during the study period. TPUs are the smallest planning units in Hong Kong's town planning system. As of the 2016 census, Hong Kong was divided into 291 TPUs, each with an average area of 3.88 km^2 and typically housing around 25,000 residents (Hong Kong Census and Statistics Department (HKCSD), 2016). During the study period, five boundary changes occurred, affecting 11 TPUs. To maintain consistency in our analysis, TPUs that experienced boundary changes were merged with adjacent ones. This consolidation process resulted in a final set of 286 units for subsequent analysis. Individual mortality data with TPU identifiers were aggregated as TPU-specific daily series of all-cause mortality counts. Daily air temperatures and relative humidity during the study period were obtained from the Hong Kong Headquarter (HKO) station, the most representative urban station with a complete dataset for the study period (H. C. Ho et al., 2020).

Hourly concentration data of ozone (O3) and respirable suspended particles (particular matters with an aerodynamic diameter smaller than or equal to 10 μm, PM10) were obtained from the 11 general stations in Hong Kong (Hong Kong Environmental Protection Department (HKEPD), 2023). Based on hourly monitoring data, the 24-hour daily

average concentration of ozone and PM10 for each station were calculated before identifying the daily average values across all 11 stations.

2.2.2. Gridded dataset of air temperature and population

Unlike traditional analyses relying solely on aggregated time series and temporal contrasts, this study employed a high-resolution gridded air temperature dataset to examine heat-mortality associations. The dataset was obtained following three steps. First, the daily gridded air temperature data across Hong Kong were extracted from the high-resolution and long-term (HLRT) daily gridded dataset, which provides daily maximum and minimum air temperatures on a 1 × 1 km grid across China from 1961 to 2019 (Qin et al., 2022). Figure A1 illustrates the spatial structures, with average daily maximum and minimum summer temperatures during the study period superimposed on the TPU boundaries. Second, the extracted dataset underwent a bias correction against the observation data from HKO through a previously documented quantile data mapping approach (Qian & Chang, 2021; Yoshikane & Yoshimura, 2023). Third, the gridded daily maximum and minimum temperature data were averaged to derive the daily mean temperature on a 1 × 1 km grid.

To accurately measure human exposure (Qi et al., 2012; Sadeghi et al., 2022), we calculated the population-weighted daily temperature for each TPU. We first resampled the original 1 × 1 km mean daily temperature into a 100 × 100 m grid through a bilinear algorithm to match the WorldPop data at 100 m resolution (Tatem, 2017). The corresponding TPU-specific daily temperature series were then derived by calculating the population-weighted average of the values of all grid cells intersecting TPU boundaries.

2.2.3. Greenspace exposure assessment

All available Landsat images with a 30 × 30 m resolution, spanning from 2005 to 2018, were acquired and processed using the Google Earth Engine (GEE) platform. Low-quality Landsat imagery including pixels affected by clouds and cloud shadows was identified based on the pixel quality assessment (QA) band. To obtain could-free imagery, affected pixels were excluded by the cloud mask provided with the QA band (Bian et al., 2020). The resulting cloud-free Landsat image collection was subsequently utilized to calculate the normalized difference vegetation index (NDVI), a widely-used index of vegetation presence and density. The NDVI equals the difference between near-infrared and visible radiation divided by the sum of the two (Tucker, 1979). The resulting index ranges between −1 and 1, with higher values indicating denser vegetation (Weier and Herring, 2000). The annual NDVI composite was calculated using the Maximum Value Compositing (MVC) technique (Holben, 1986). It was then used to estimate the average NDVI of each grid cell over the study period (Figure A2). By averaging the values of all grid cells within the TPU boundary, a long-term TPU-specific NDVI was produced, which was used as a proxy of greenspace exposure at the area level.

The total and factions for three types of greenspace at 30-m resolution were quantified, using the GlobeLand30 in 2010, including forest, shrub and grassland (Figure A3). The GlobeLand30 dataset is the first open-access, high-resolution map of Earth's land cover data developed and released by the National Geomatics Center of China and comprises ten types of land cover (J. Chen et al., 2017). TPU-specific exposure to the total and specific types of greenspace were measured by the proportion of the total and each type of greenspace within a TPU. Due to the minimal shrub in Hong Kong (Figure A3), this study mainly focused on two specific vegetation types: forest and grassland.

In addition to the area-level greenspace exposure, population-weighted exposure metrics were calculated within various buffer distances ranging from 200 m to 4 km in each TPU. For the NDVI-based exposure metric, first the original 30 m annual NDVI composite was resampled to a 100 m resolution to match the annual WorldPop data from 2005 to 2018. Then, the annual population-weighted NDVI-based exposure was calculated within varying buffer sizes for each TPU following Eq. (1) (Chen et al., 2022a). The resulting annual exposure metrics were averaged over the study period to represent the TPU-specific NDVI-based exposure. For exposure metrics based on the land cover map, first the total and then the factions for three types of greenspace were extracted from the GlobeLand30 in 2010. Data were then resampled on a 100 × 100 m grid to match the corresponding population data in the same year. The population-weighted exposure was calculated to the total and different types of greenspace within various buffer distances following Eq. (1).

$$GE(d) = \frac{\sum_{i=1}^{n} Pop_i \times GE(d)_i}{\sum_{i=1}^{n} Pop_i}$$

where Pop_i represents the population of the grid i, and $GE(d)_i$ represents the corresponding NDVI or the proportion of total or a specific type of greenspace (i.e., forest, shrub, and grassland) within a buffer distance of d meters for that grid ($i = 200, 400, 600, \ldots, 4000$ m); n donates the total number of grids within a given unit (i.e., a TPU in this study), and $GE(d)$ denotes average greenspace exposure per person for that unit at a buffer distance of d meters.

2.3. Statistical analysis

A novel CTS design was used to assess the association between temperature and total mortality across small areas, fitting the TPU-specific series by a conditional Poisson regression. The CTS modeling framework incorporates the self-matched structure in case-only design into a classical time series form and is well suited for small-scale epidemiological studies (Gasparrini, 2021). Here, the daily mortality of each TPU was defined as the event-type outcome and was linked to the corresponding daily temperature of that unit. A bi-dimensional spline distributed lag nonlinear model (DLNM) with a cross-basis term was fitted, accounting for the nonlinear exposure–response associations and lagged dependencies simultaneously. Specifically, the exposure–response curve was modeled using a natural cubic spline with two internal knots at the 50th and 90th percentiles of summer temperatures, and the lagged effects of heat, using a natural spline with one knot placed on the log scale up to 3 days. The model also accounts for temporal trends, using a matching stratum defined by year, month and TPU, indicators of days of a week and holidays, natural splines of days of the year with 4 degrees of freedom, and an interaction term with year indicators, as done in a past study (Gasparrini, 2022). The bi-dimensional temperature-lag response curve was then reduced to a one-dimensional overall temperature-mortality association by cumulating the risk over the lag dimension. The minimum mortality temperature (MMT) was identified, corresponding to the temperature value for the minimum temperature-mortality risk. Mortality risks under extreme heat were then summarized by computing the relative risks (RR) and related 95 % CIs at the 99th temperature percentiles versus the MMT, respectively.

The CTS models could be further extended by introducing an interaction term with time-invariant terms to investigate the effect modifications. In this instance, a linear interaction was included between the cross-basis temperature and each greenspace exposure metric into the CTS models to separately explore the effect modification of total and specific types of greenspace. Based on univariate interaction models, the pooled exposure–response curves at the lowest and highest quartiles of each greenspace exposure metric were first predicted for extracting the RRs under extreme heat (at the 99th temperature percentile versus the MMT). Next, the p-value between the lowest and highest quartiles of each greenspace exposure metric was calculated, using the Wald-test to explore the significance of the effect modification for each metric. In addition, the difference in the temperature-mortality associations was predicted, expressed as the ratio of RRs, between the lowest and highest quartiles of each greenspace exposure metric at the 99th temperature percentile. The ratio of RRs was used as a proxy of the strength of effect modification for each metric, following a previously described method

(Pascal et al., 2021; Qiu et al., 2021; Schinasi et al., 2018). A higher ratio of RRs indicates stronger effect modifications. The significance and strength of effect modifications of the population-weighted exposure was also explored for total and specific types of greenspace at various buffer distances, ranging from 200 m to 4 km. The estimated results allowed for an identification of the optimal exposure distance to the total and each type of greenspace. Finally, the ratios of RRs for the paired area-level exposure and the population-weighted exposure within the optimal distance for the total and specific types of greenspace were also explored. The Wald test was used to explore if there was a significant difference between two sets of exposure metrics.

Spearman's correlation analyses were adopted to identify potential confounding effects of the socioeconomic status (SES) and blue space exposure, based on their correlations with greenspace exposure metrics. A set of variables, including age, education, income, and distance to coast were selected as proxies of SES and that of blue space exposure following a literature review (Burkart et al., 2016; Song et al., 2022). Details on data sources and definitions are provided in the appendix (Table A1). Sensitivity analyses were then performed by including each SES variable and the variable of blue space exposure into the univariate interaction model as a potential modifier, and by including daily relative humidity, daily concentration of O3 and PM10 at 0–1 lag days to control the confounding effects of other time-varying variables. All analyses were performed in R v4.3.1. The CTS models were fitted using the ***dlnm*** and ***gnm*** packages. The Wald test was performed using the *metaphor* package. Two-tailed p-value < 0.05 was considered to be statistically

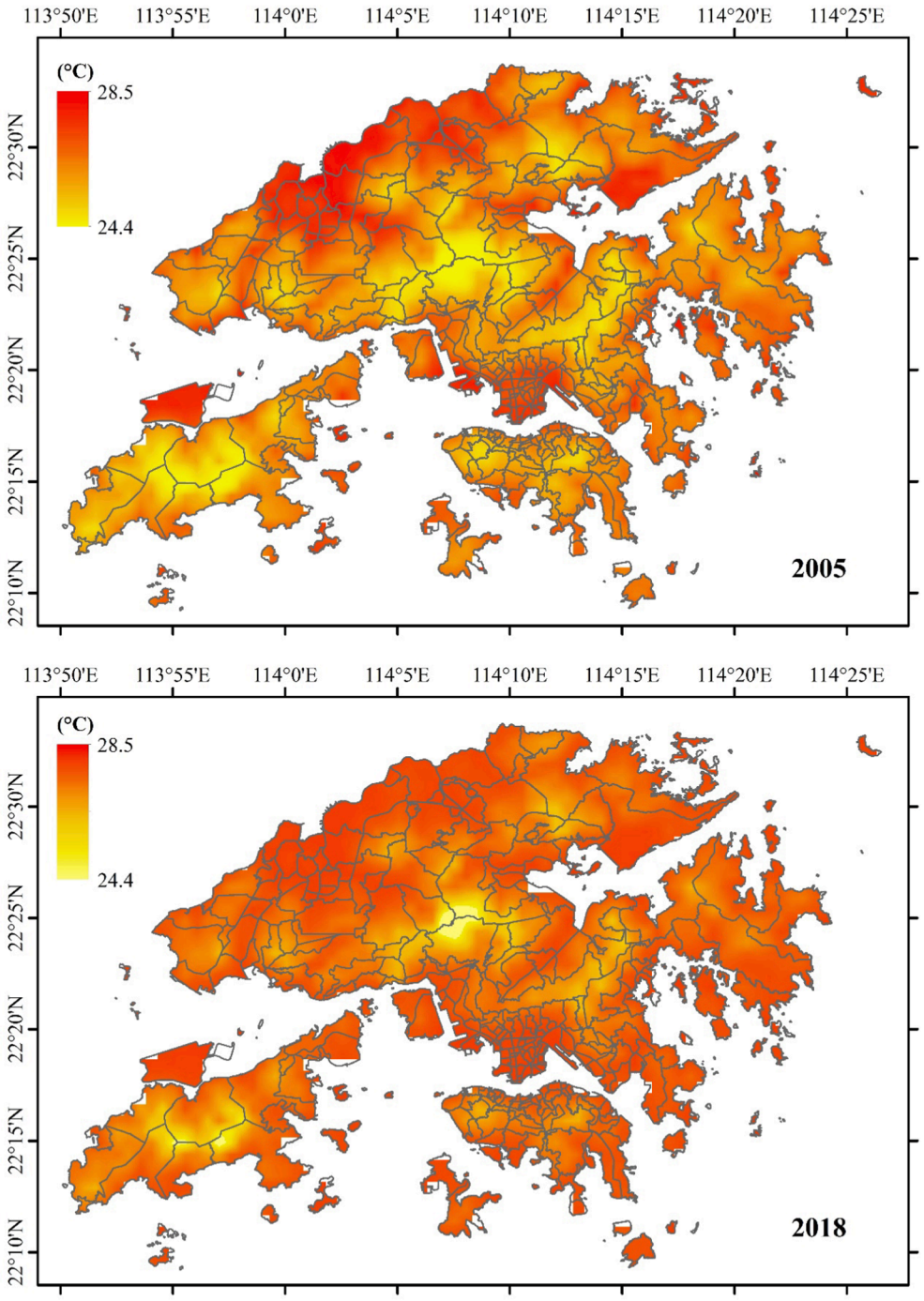

Fig. 1. Average population-weighted summer temperature (°C) in 2005 (top) and 2018 (bottom) at a 100 m × 100 m grid overlaid by the boundaries of 286 TPUs.

significant.

3. Results

3.1. Characteristics of study area

The analysis included 221,919 deaths from all causes across 286 TPUs during the summer months (June to October) from 2005 to 2018. Of these, 213,505 deaths (over 95 % of all-cause mortality) were attributed to non-accidental diseases. The average daily mean temperature was 28.0 °C, ranging from 18.9 °C to 32.2 °C. The 99th percentile of temperature distributions was 31.2 °C. The mean daily relative humidity was 77.78 %. The mean daily concentrations of air pollution were 41.73 μg/m3 for O3 and 44.69 μg/m3 for PM10 at 0–1 lag days. Fig. 1 shows the average population-weighted summer temperatures at a 100 m × 100 m grid in the two years. As expected, the summer temperature exhibits a geographical gradient, with higher values in densely populated areas. Table 1 provides a statistical summary of NDVI and proportions of total greenspace, forest land and grassland at the TPU level.

The overall cumulative temperature-mortality relationship estimates have a minimum value at 26.7 °C, corresponding to the MMT. Significantly increased risks were observed under extreme heat, with RRs being 1.040 (95 %CI: 1.009,1.072) at the 99th percentile (31.2 °C), compared to MMT.

3.2. Effects of various area-level greenspace exposure metrics on heat-mortality associations

The upper panel in Fig. 2 displays the exposure–response curves predicted at the lowest and highest quartiles of each area-level greenspace exposure metric—namely, NDVI and proportions of total and specific types of greenspace—using the univariate interaction models. TPUs at the highest quartile of area-level exposure to total greenspace show a lower heat-related mortality risk (indicated with the red vertical dot-dashed line) compared to TPUs at the lowest quartile, with the RR rising from 1.00 (95 %CI: 0.94, 1.06) to 1.05 (95 %CI: 1.02, 1.08) for NDVI, and 0.99 (95 %CI: 0.93, 1.06) to 1.06 (95 %CI: 1.02, 1.10) for the proportion of total greenspace, albeit not significant considering the returned p-values > 0.05. A similar pattern can be observed for the forest land with more apparent effect modifications under extreme heat, with the RR rising from 0.98 (95 %CI: 0.92, 1.05) to 1.06 (95 %CI: 1.03, 1.10) for the highest to lowest quartiles (p-value = 0.037), while for grassland no differences were found in the heat tail.

The lower panel of Fig. 2 shows the ratio of RRs between the lowest and highest quartiles of different exposure metrics—namely, NDVI and proportions of total and specific types of greenspace—over the whole range of summer temperatures. The ratio of RRs indicates the difference in the temperature-mortality associations for the highest and lowest quartiles of greenspace exposure, and can be interpreted as a measure of the strength of the effect modifications for each area-level greenspace exposure metric. In this instance, the area-level exposure to total greenspace presents a promising but insufficient effect to limit the impacts of extreme temperature, with the ratio of RRs being 1.170 (95 %CI: 0.958, 1.429) for NDVI, and 1.001 (95 %CI: 1.000, 1.002) for the proportion of total greenspace under extreme heat. For specific vegetation types, similar results were observed, with the ratio of RRs being 1.001(95 %CI: 1.000,1.002) for forest land and 1.001 (95 %CI: 0.996,1.005) for grassland under extreme heat.

Table 1
Statistical summary of NDVI and proportions of total greenspace, forest land and grassland at the TPU level.

Metrics	Mean	SD	Min	P25	P50	P75	Max
NDVI	0.46	0.18	0.10	0.32	0.48	0.61	0.74
% total greenspace	52.88	38.36	0.00	10.00	61.07	91.33	100.00
% forest land	46.80	35.95	0.00	7.18	47.86	82.24	100.00
% grassland	4.11	8.23	0.00	0.00	0.00	4.77	54.39

3.3. Effects of population-weighted greenspace exposure at varying buffer distances on heat-mortality associations

Fig. 3 provides a graphical representation of the significance and strength of effect modifications for the population-weigthed exposure to total and specific types of greenspace within a varying buffer distance under extreme heat, expressed by the RRs (the upper panel) and the ratio of RRs (the lower panel) between the lowest and highest quartiles of each exposure metric at the 99th temperature percentile. The population-weighted NDVI demonstrates significant effect modifications on the heat-mortality relationship across buffer distances ranging from 800 m to 1400 m (p-values < 0.05). The optimal effect is observed at approximately 1000 m, with a ratio of RRs being 1.424 (95 %CI: 1.038,1.954). In other words, people living in areas corresponding to the lowest quartile of the optimal distance-based NDVI could face a heat-related mortality risk 1.424 times higher than those living in areas with the highest quartile.

A similar scale of effects was observed for the population-weighted proportion of total greenspace and that of forest land, with significant effect modifications on heat-mortality associations within a buffer distance ranging from 800 m to 1400 m, and 800 m to 1600 m, respectively. The presence of total greenspace and forest land also shows similar gradient regarding the strength of effect modifications. A sharp increase was observed in the curves of the ratio of RRs for both with an increase of the buffer distance to 1000 m, followed by a decrease beyond 1000 m. The curve of the ratio of RRs for grassland presents a sharp decrease as the buffer distance rises, though the effect remains insignificant for buffers of different sizes, ranging from 200 m to 4000 m, as confirmed by the returned p-values > 0.05.

3.4. Difference between the effects of area-level and population-weighted greenspace exposure within the optimal distance

Table 2 shows the ratio of RRs for the lowest to highest quartiles of greenspace exposure, depending on specific metrics estimated at the area level and within the optimal distance. The returned p-values of the difference in the ratios of RRs between each paired greenspace exposure metric suggested little difference in the effect modifications between area-level NDVI and population-weighted NDVI within the optimal distance (p-value > 0.05). In contrast, a marked difference was observed in terms of the paired area-level and population-weighted exposure to total greenspace and forest land under extreme heat (p-values < 0.05). No significance was established for grassland.

3.5. Results of correlation and sensitivity analyses

According to results of Spearman's correlation analyses (Figure A4), NDVI, the proportion of total greenspaces, and the proportion of forest land were highly correlated with each other (Spearman correlation $r > 0.88$). However, no explicit association was observed for the three indices with the proportion of grassland ($r < 0.28$). There was a weak to non-explicit association between socio-economic variables and greenspace exposure indices, as well as between the variable of blue space exposure and greenspace exposure indices ($r < 0.33$). In addition, no significant difference was observed between the RR curves of the high and low SES levels considering the three selected variables (Figure A5). There was little evidence of significant effect modifications of SES variables under extreme heat (at the 99th temperature percentile, 31.2 °C), as confirmed by returned p-values > 0.05 of Wald-test (Table A2). Therefore, the confounding effect of each SES variable would be, if present, minimal to that of each greenspace metric. Similar results were

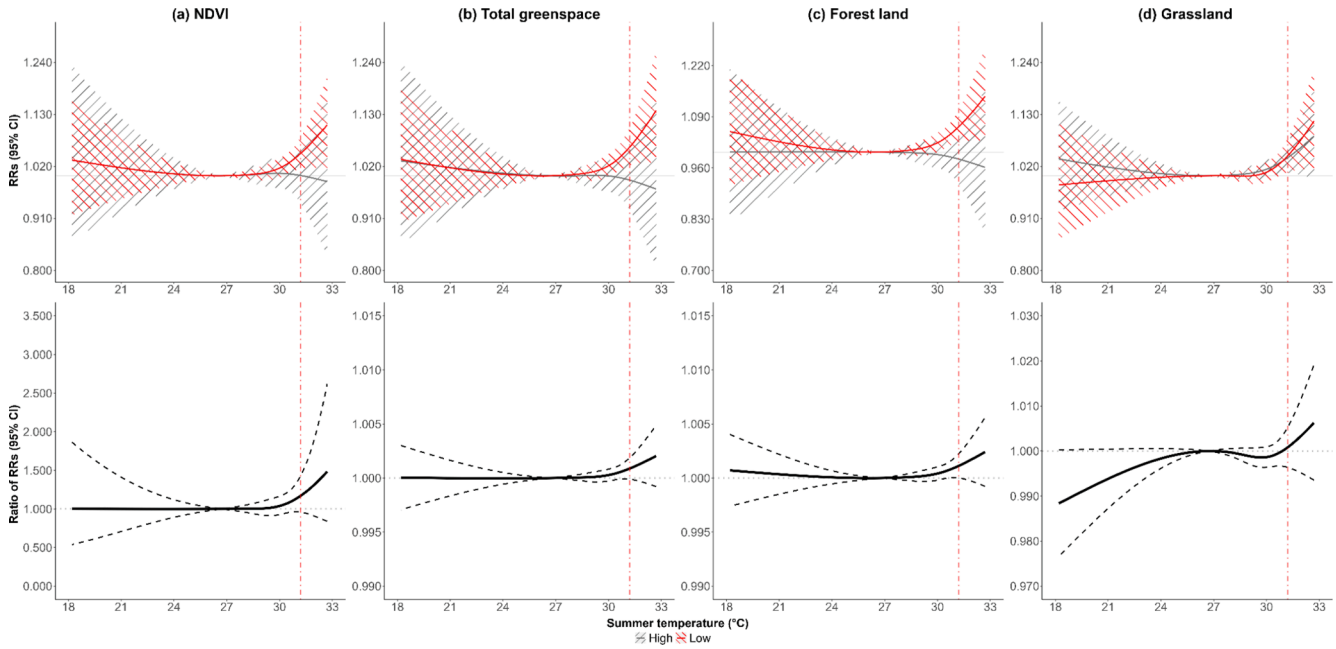

Fig. 2. The relative risks (RRs) (the upper panel) and the ratio of RRs (the lower panel) between the lowest and highest quartiles of each area-level greenspace exposure metric over the whole summer temperature, with 95 % confidence intervals. The area-level greenspace exposure was assessed by the average value of a) NDVI; and the proportion of b) Total greenspace; c) Forest land; d) Grassland for each TPU. The RRs and the ratio of RRs under extreme heat (at the 99th temperature percentile, 31.2 °C) were indicated in the red dot-dashed line.

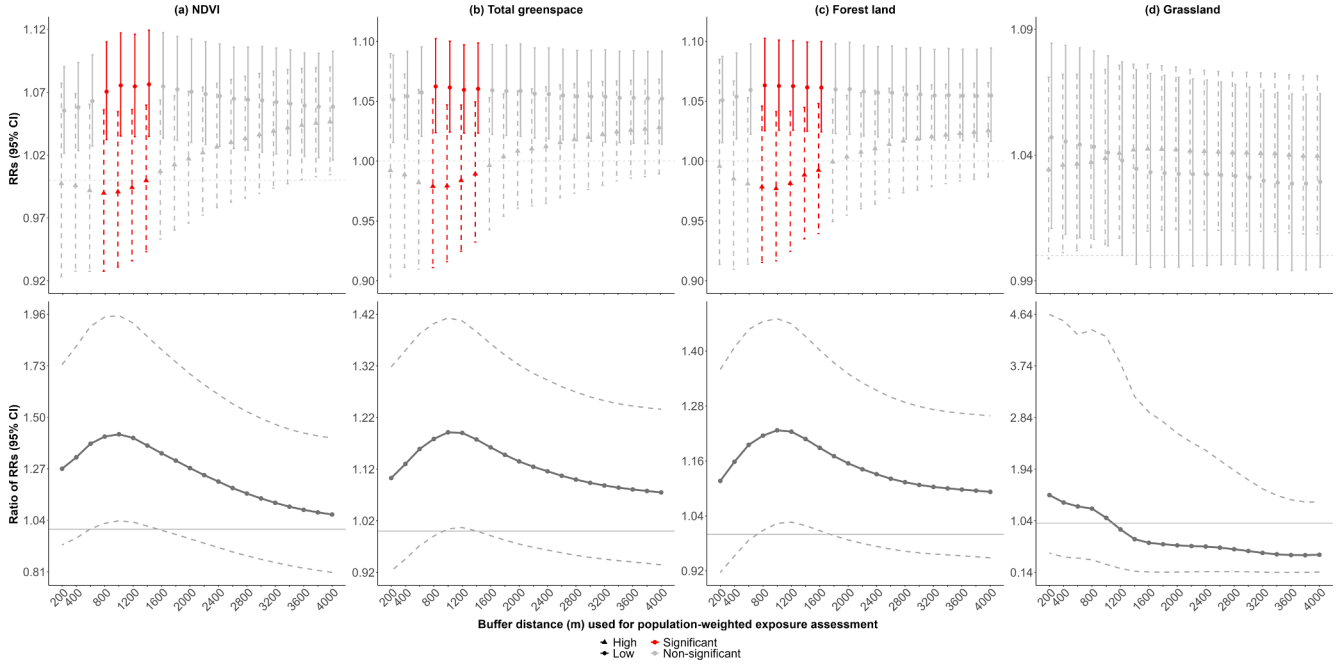

Fig. 3. The relative risks (RRs) and the ratio of RRs between the lowest and highest quartiles of each population-weighted greenspace exposure metric within a buffer distance ranging from 200 m to 4000 m under extreme heat (at the 99th temperature percentile, 31.2 °C), with 95 % confidence intervals. The greenspace exposure was assessed based on population-weighted metric in terms of: a) NDVI; b) Total greenspace; c) Forest land; d) Grassland.

observed for the variable of blue space exposure (Figure A5 & Table A2).

Sensitivity analyses also show that similar effect modifications of exposure to total and specific types of greenspace were observed after controlling for relative humidity and concentrations of O3 and PM10, for both area-level indices and population-weighted indices at varying buffer distances (Figs. A6 & A7, Table A3). This is the indication of the robustness of the analyses.

4. Discussion and conclusion

This study has comprehensively characterized the health benefit of greenspace exposure protection from heat by using high-resolution temperature data and exploring the effects of different types of greenspaces. This study is also unique in having simultaneously assessed the effect modifications of area-level greenspace exposure, as well as population-weighted greenspace exposure within varying buffer

Table 2
The ratio of relative risks (RRs) between the lowest and highest quartiles of each paired greenspace exposure metrics at the area level and within optimal exposure distance under extreme heat, and the *p-value* for the difference in the ratio of RRs between each paired greenspace exposure metrics.

Variables	Exposure metrics	Ratio of RRs (95 % CI)	*p-value* for the difference in Ratios of RRs
NDVI	Area level	1.170(0.958,1.429)	0.304
	Within optimal distance	1.424(1.038,1.954)	
Total greenspace	Area level	1.001(1.000,1.002)	0.045
	Within optimal distance	1.191(1.004,1.413)	
Forest land	Area level	1.001(1.000,1.002)	0.028
	Within optimal distance	1.227(1.024,1.470)	
Grassland	Area level	1.001(0.996,1.005)	0.494
	Within optimal distance	1.488(0.477,4.638)	

Note: Ratio of RRs is short for the ratio of relative risks between the lowest and highest quartiles of each greenspace exposure metric. Exposure metrics at the area level refer to the mean value of NDVI or the proportion of the total or specific type of greenspace within each TPU, while those within optimal distance indicating a population-weighted mean value of NDVI or the proportion of the total or specific type of greenspace at the optimal buffer distance within each TPU. The optimal distance was 1000 m for NDVI, the proportion of total greenspace, and the proportion of forest land, and 200 m for the proportion of grassland under extreme heat (at the 99th temperature percentile, 31.2 °C).

distances.

Variations in heat-related mortality were established for different vegetation types. The RRs were significantly higher in areas categorised as being in the lowest quartile of forest land exposure, although the between-group difference was limited in terms of the ratio of RRs. However, such variation was not significant in terms of grassland exposure across TPUs. This is probably because, in addition to evaporative cooling, shading from trees can immdediately intercept solar radiation, and thus create local cool areas beneath the tree canopies (Oke, 1989). An empirical study in Hong Kong found that trees were more effective than grass surfaces in cooling pedestrian areas (Ng et al., 2012). Another possible explanation is that the amount and size of grassland in Hong Kong is too small to provide residents with enough open public space. Previous studies indicated that people were less likely to visit or use small-size greenspaces, which may constrain the health benefits of ground vegetation in Hong Kong (Ekkel & De Vries, 2017).

A novel finding is the variation in the health benefits of population-weighted greenspace exposure against heat at varying buffer distances. The results are unique in showing the buffer distance that is best suited for representing the pathway linking greenspace to heat health risk reduction, and how it may vary by exposure metrics and specific types of greenspace. The effect modifications were found to be strongest when considering exposure to the nearby total greenspace and forest land. There appears to be no empirical support from past studies for a specific cut-off value for distance that could represent the greenspace-heat health pathways. However, our findings are consistent with other studies that report significant protective associations between physical health and nearby greenspaces (Browning & Lee, 2017; Gullón et al., 2023; Hajna et al., 2023).

The exact mechanisms that lead to the changing effects of greenspace at varying buffer distances cannot be fully elaborated on. The underlying reasons are connected with direct and indirect pathways linking greenspace to health impacts of heat. Greenspaces are thought to decrease heat mortality risk directly via cooling processes. A few studies have reported the extension of the cooling effect of a green area beyond its boundary, indicating a general cooling effect rather than only localized cooling (Bowler et al., 2010). Therefore, temperatures for local residents at a specific site would be affected by surrounding greenspace within a certain radius of their location. Our findings suggest that a buffer distance of 1000 m is best suited for representing the pathway linking greenspace exposure to death risk from heat. Ziter et al. (2019) observed a more apparent cooling effect of the canopy at broader scales. This finding corresponds to the attenuated effect modifications of greenspace at small buffer distances shown in Fig. 3.

In addition, vegetation might also affect air movements and heat exchange (Bonan, 1997). This effect can be expected to depend on the type of vegetation. In terms of vegetation's wind sheltering effect (Gunawardena et al., 2017), trees may block air ventilation and retain warm air beneath the canopies, thus probably offsetting the localized cooling effects from evapotranspiration and shading; in contrast, an open grass field that provides low resistance to air flow may promote cooling by convection (Bowler et al., 2010). Such difference in the cooling mechanism may partially explain the lower values at the left tail of the curve of forest land exposure, and the difference in the trend of forest and grassland in the bottom panel of Fig. 3.

For the indirect pathways, nearby trees and greenspaces are more frequently visited by residents than distant ones (Browning & Lee, 2017; Fouad et al., 2023; Schindler et al., 2022; Wong, 2009). More frequent visits can lead to better mental and physical health via increases in physical activity, reduction in stress, and mitigation of heat and air pollution exposure (better thermoregulation and physiological mechanisms to resist heat impacts) (Lim, 2020). Therefore, the drop of visits to distant greenspaces and consequently reduced health benefits may lead to a decline in the effect modifications of greenspace exposure at a large buffer distance shown in the bottom panel of Fig. 3.

Comparisons of paired area-level and population-weighted greenspace exposure demonstrate that the estimates of the effect modification of greenspaces are sensitive to the choice of metrics. As with the traditional approaches, the effect modifications of greenspace on heat-mortality associations were mainly estimated based on the area-level exposure metrics regardless of population distribution or the effects of varying buffer distances (Burkart et al., 2016; Son et al., 2016). Previous studies had reported insignificant effect modifications of greenspaces on heat impacts by using area-level metrics (Gronlund et al., 2016; Song et al., 2022). These findings raise concerns about the potential for exposure misclassification in their deprivation of the exposure–response association for the study population. The absence of effect modifications may simply reflect exposure misclassifications (Gronlund et al., 2016).

A significant disparity was observed in the estimated effects of exposure to total greenspace and forest land by using area-level and population-weighted indices within the optimal buffer distances. Findings indicate a possibility of a more significant pathway of population-weighted exposure to nearby trees and greenspaces, besides area-level exposure. This pathway has important implications for population-level heat mitigation strategies. Planting trees or greening should happen within walkable distances (around 1000 m) to local residents, in addition to the purposeful increase of area-level presence of vegetation.

Meanwhile, the limited effect modifications of greenspace exposure at small buffer distances suggest that urban greening should occur at a broader scale rather than very close to residents. The findings challenge some proposed strategies for improving general health by having greenspace within a five-minute walk (Blanck et al., 2012) or a buffer of 500 m or less (Browning et al., 2022) to residents. However, the findings have important implications for heat mitigation strategies through urban greening. First, planting trees or greening in targeted locations where people live—such as individual or clusters of trees adjacent to a house or yard, or along a well-used walking path—may benefit different domains of physical health (Rojas-Rueda et al., 2019). However, decision makers need to understand that protective effects against heat may be small if the surrounding area has a low canopy and is less vegetated.

Second, as the compact building footprints in high-density cities probably limit the ability of tree canopies to flourish, greenspaces may not be directly accessible to all those who might benefit during periods of very high temperatures (Ziter et al., 2019). According to our findings, nearby greenspace at a broader scale may help buffer declined health benefits due to the shortage of vegetation cover at a finer scale, allowing for more flexible planning and design solutions for urban greening in compact cities, like Hong Kong.

As one of the first attempts to explicitly link heat health risk reduction to greenspace exposure considering the varying effects by vegetation type and at buffers of different sizes, the empirical findings presented in this paper have some limitations. Firstly, this study computed the effect estimates, using aggregated data at small-area level. The findings are potentially susceptible to the "ecological fallacy". Future studies are thus advised to explore the impacts of the size of analysis units (Kwan, 2012). Second, heat-related mortality risks are affected by various factors, residual confounding cannot be fully ruled out. Genetic factors, accidents, or injuries could be among these factors and merit further investigation once relevant data become available. Other meteorological factors, including precipitation, atmospheric pressure, and wind directions, were not included due to data unavailability for the entire period. This limitation presents opportunities for future research. Third, to maintain sufficient statistical power, we did not differentiate the effect modifications of greenspace exposure by cause of death or age group. Nonetheless, given a larger dataset, such stratification would be worth considering in further research. Fourth, the results were computed over a relative long study period. The temporal variations in risks and the estimated effects were not accounted for in the present study but all have significant potential to be a focal point for continued work. Fifth, while this study incorporated the most recent insights in greenspace exposure assessment (Chen et al., 2022a; Chen et al., 2022b), the proliferation of new data sources and emerging technologies offer potential for further refinement. The Green View Index, derived from street-view imagery, provides pedestrian-level perspectives of urban greenery, complementing traditional aerial measures (R. Wang et al., 2019). Urban forest composition and canopy structure, particularly tree species diversity, merit consideration due to their varying cooling efficiency and allergenic potential.. Additional factors include greenspace size, shape and spatial patterns (Kong et al., 2014; Masoudi et al., 2019), as well as the actual greenspace utilization (James et al., 2015) and the combined effects of these factors.

Moreover, this study derived risks at low and high levels of greenspace exposure through univariate models. Other factors that might explain the spatial differences in heat-mortality associations across analysis units (TPUs) were not accounted for, such as the differential air pollution levels and topological conditions across space. Further development of more advanced models thus need to disentangle the effect modifications of various space-varying factors, including air pollution exposure and elevation. Additionally, prior studies have documented that the health benefits of greenspace exposure can vary depending on the specific health outcomes being studied (Yang et al., 2021). Therefore, there is uncertainty regarding the generalization of our findings to other health outcomes, such as heat-related morbidity. Lastly, although the analysis made use of high-resolution temperature data linked with small-area information, these were produced by machine learning approaches. In this context, uncertainty was neither quantified nor considered in the analysis.

In conclusion, nearly all extant small-scale studies that have investigated the effect modifications of greenspace on the heat-mortality association have focused primarily on the area-level metrics of greenspace regardless of the population distribution and the scale of effects. This paper extended existing research by demonstrating that vegetation types, population distribution, and distance to greenspaces have important roles to play in heat-mortality associations. Specifically, the effects of greenspace are most significant at a buffer distance of 1000 m under extreme heat, independent of metrics used but vary by vegetation type. The findings provide insight into the optimal buffer sizes for representing the specific health pathway between greenspace and heat impact mitigation. Furthermore, these findings may provide insights into the reason for non-significant results observed in previous studies that employed area-level metrics only, irrespective of the population distribution or the scale of effect (Gronlund et al., 2016; Madrigano et al., 2013; Xu et al., 2013). The authors believe that particular interventions in residential greenspace within a walkable distance (around 1000 m) could effectively reduce heat exposure and vulnerability, thereby, decrease the likelihood of mortality from heat. If these findings are replicated, such implications will be of importance to urban planners and designers as they seek to achieve maximal health benefits through informing measures of modifiers to specific pathways and threshold effects for each.

5. Author statement

Contributions of authors were as follows: **J. S.:** conceptualization, data curation, formal analysis, investigation, methodology, software, visualization, writing-original draft, writing-review and editing, funding acquisition; **A. G.:** methodology, software, writing-review and editing, funding acquisition; **D. W.:** data curation, funding acquisition; **Y. L.:** data curation, methodology, funding acquisition; **K. H.:** data curation, funding acquisition; **T. F.:** writing-review and editing; **N. M:** methodology, writing-review and editing, funding acquisition.

CRediT authorship contribution statement

Jinglu Song: Writing – review & editing, Writing – original draft, Visualization, Software, Methodology, Investigation, Funding acquisition, Formal analysis, Data curation, Conceptualization. **Antonio Gasparrini:** Writing – review & editing, Software, Methodology, Funding acquisition. **Di Wei:** Funding acquisition, Data curation. **Yi Lu:** Methodology, Funding acquisition, Data curation. **Kejia Hu:** Funding acquisition, Data curation. **Thomas B. Fischer:** Writing – review & editing. **Mark Nieuwenhuijsen:** Writing – review & editing, Methodology, Funding acquisition.

Declaration of competing interest

The authors declare that they have no known competing financial interests or personal relationships that could have appeared to influence the work reported in this paper.

Data availability

Data will be made available on request.

Acknowledgement

The study was supported by the National Natural Science Foundation of China (grant numbers: 42007421 to J.S., 42001013 to K.H.), Research Development Fund of XJTLU (grant number: RDF-19-02-13, to J.S.), Medical Research Council-UK (grants numbers: MR/R013349/1 and MR/V034162/1, both to A.G.), General Research Project Fund of Hong Kong Research Grants Council (grant number: CityU11207520, to Y.L.), the Fundamental Research Funds for the Central Universities, HUST (grant number: 2021JYCXJJ009, to D.W.), Zhejiang Provincial Natural Science Foundation of China (grant number: Y23D050006, to K.H.), Spanish Ministry of Science and Innovation and State Research Agency through the "Centro de Excelencia Severo Ochoa 2019-2023" Program (grant number: CEX2018-000806-S, to N.M.) and the "Generalitat de Catalunya through the CERCA Program" (to N.M.).

We thank the efforts of the Hong Kong Census and Statistics Department (HKCSD) in collecting and processing the census and mortality data.

Appendix A

Table A1
Descriptive statistics of socioeconomic variables and the variable of blue space exposure in Hong Kong.

Variables	Mean	SD	Min	P25	P50	P75	Max
% older adults [1]	14.57	3.81	6.15	11.46	14.57	17.38	24.05
% low education [2]	9.1	2.91	4.51	7.01	8.67	10.7	20.71
% low income [3]	3.16	0.89	0.95	2.64	3.09	3.45	8.3
Distance to coast [4] (m)	1631.58	1833.62	1.42	352.12	946.66	2144.72	8310.27

Note: Data for each variable were obtained from the 2006 and 2016 Hong Kong censuses (Hong Kong Census and Statistics Department (HKCSD), 2006, 2016). The smallest census units with available data in the two rounds of censuses were large TPUs, in which adjacent TPUs with small populations were merged into a large unit. Owing to the limited inland water body in Hong Kong, the distance to coast of each TPU was selected as a proxy for blue space exposure and was represented by the shortest Euclidean distance from the population-weighted centroid of each TPU to the coastlines. The population data were obtained from the WorldPop dataset (100 m × 100 m). The coastlines of Hong Kong were obtained from the iB5000 Topographical Dataset of the Hong Kong Lands Department (2014).
[1] Percent of people aged > 65 years.
[2] Percent of people aged > 15 years with educational attainment only at primary school or below.
[3] Percent of the working population with monthly income below the poverty line (i.e., HKD$2000 in 2006 and HKD$4000 in 2016, according to the poverty indicator in Hong Kong (Hong Kong Census and Statistics Department (HKCSD), 2023)).
[4]Population-weighted distance to the coastline.

Table A2
Relative risks (RRs) (95 % CI) for mortality associated with the lowest and highest quartiles of each variable of socioeconomic status (SES) and the variable of blue space exposure, the *p*-value for a likelihood test, and the ratio of RRs (95 % CI) between the two quartiles.

Variables of SES	RRs (95 % CI) (99th vs. MMT)		Ratio of RRs (95 % CI)	*p*-value for inter-quartile difference
	Lowest Quartile	**Highest Quartile**		
% older adults [1]	1.055 (1.002,1.111)	1.052 (1.012,1.093)	1.001 (0.991,1.010)	0.923
% low education [2]	1.052 (0.993,1.113)	1.053 (1.017,1.089)	1.000 (0.995,1.005)	0.9809
% low income [3]	1.060 (1.015,1.107)	1.051 (1.017,1.086)	1.011 (0.965,1.059)	0.7658
Distance to coast[4] (m)	1.070 (1.028,1.114)	1.046 (1.011,1.081)	1.001 (1.000,1.003)	0.3863

Note: Ratio of RRs is short for the ratio of relative risks between the lowest to highest quartiles of each variable. Data for each SES variable were obtained from the 2006 and 2016 Hong Kong censuses (Hong Kong Census and Statistics Department (HKCSD), 2006, 2016). The smallest census units with available data in the two rounds of censuses were large TPUs, in which adjacent TPUs with small populations were merged into a large unit. Owing to the limited inland water body in Hong Kong, the distance to coast of each TPU was selected as a proxy for blue space exposure and was represented by the shortest Euclidean distance from the population-weighted centroid of each TPU to the coastlines. The population data were obtained from the WorldPop dataset (100 m × 100 m). The coastlines of Hong Kong were obtained from the iB5000 Topographical Dataset of the Hong Kong Lands Department (2014).
[1] Percent of people aged > 65 years.
[2] Percent of people aged > 15 years with educational attainment only at primary school or below.
[3] Percent of the working population with monthly income below the poverty line (i.e., HKD$2000 in 2006 and HKD$4000 in 2016, according to the poverty indicator in Hong Kong (Hong Kong Census and Statistics Department (HKCSD), 2023)).
[4]Population-weighted distance to the coastline.

Table A3
The ratio of relative risks (RRs) between the lowest and highest quartiles of each paired greenspace exposure metrics at the area level and within optimal exposure distance under extreme heat after controlling for the effects of daily relative humidity, O_3 and PM_{10} concentrations at 0–1 lag days, and the p-value for the difference in the ratio of RRs between each paired greenspace exposure metrics.

Variables	**Exposure metrics**	**Ratio of RRs (95 % CI)**	***p-value* for the difference in Ratios of RRs**
NDVI	Area level	1.173(0.961,1.433)	0.252
	Within optimal distance	1.463(1.062,2.017)	
Total greenspace	Area level	1.001(1.000,1.002)	0.043
	Within optimal distance	1.194(1.006,1.416)	
Forest land	Area level	1.001(1.000,1.002)	0.027
	Within optimal distance	1.229(1.025,1.473)	
Grass land	Area level	1.001(0.996,1.005)	0.474
	Within optimal distance	1.518(0.485,4.750)	

Note: Ratio of RRs is short for the ratio of relative risks between the lowest and highest quartiles of each greenspace exposure metric. Exposure metrics at the area level refer to the mean value of NDVI or the proportion of the total or specific type of greenspace within each TPU, while those within optimal distance indicating a population-weighted mean value of NDVI or the proportion of the total or specific type of greenspace at the optimal buffer distance within each TPU. The optimal distance was 1000 m for NDVI, the proportion of total greenspace, and the proportion of forest land, and 200 m for the proportion of grassland under extreme heat (at the 99th temperature percentile, 31.2 °C).

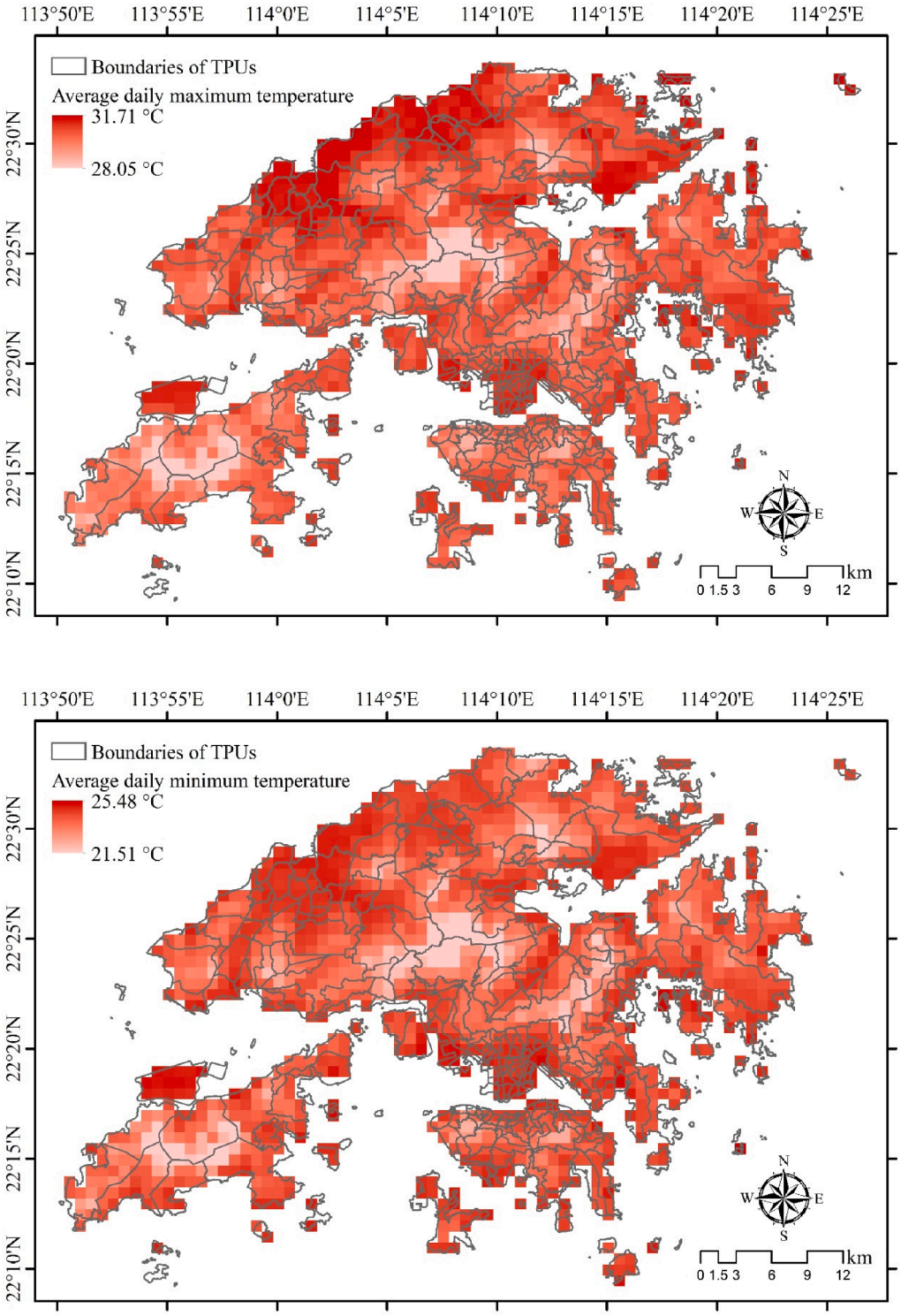

Fig. A1. Average summer temperature during 2005 to 2018 at a 1 × 1 km grid of Hong Kong, overlaid with the boundaries of the 286 TPUs.

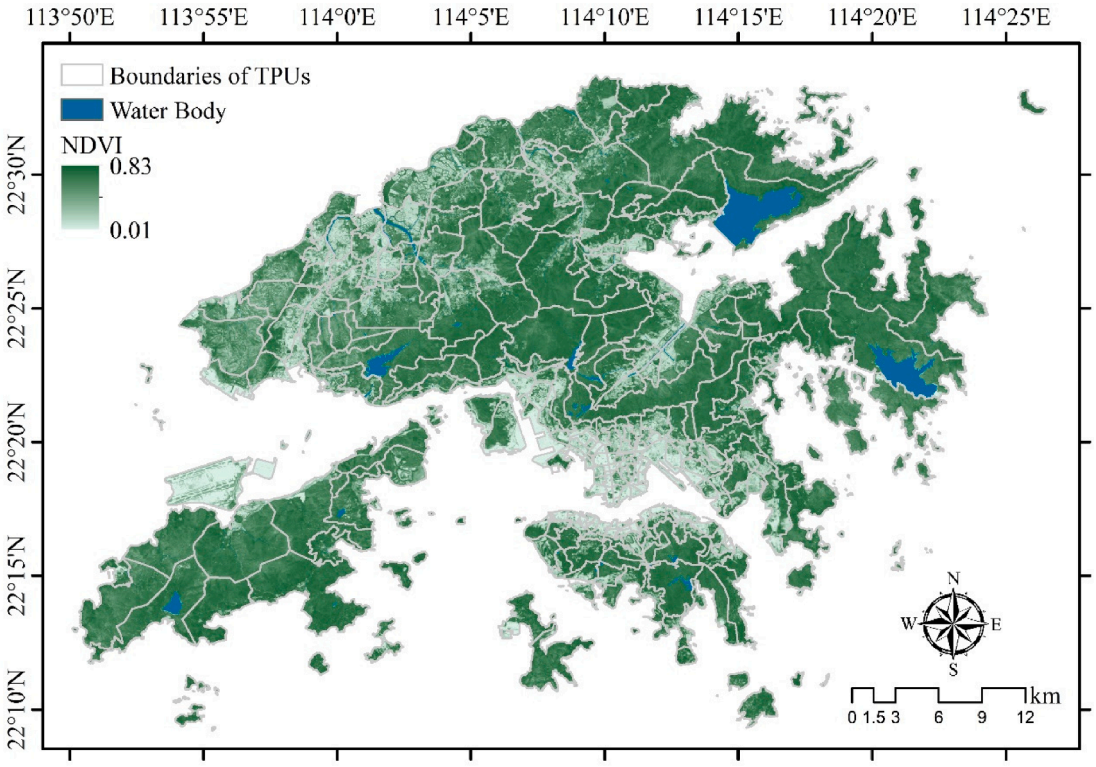

Fig. A2. Average values of NDVI during 2005 to 2018 at a 30 × 30 m grid of Hong Kong, overlaid with the boundaries of the 286 TPUs based on Landsat images.

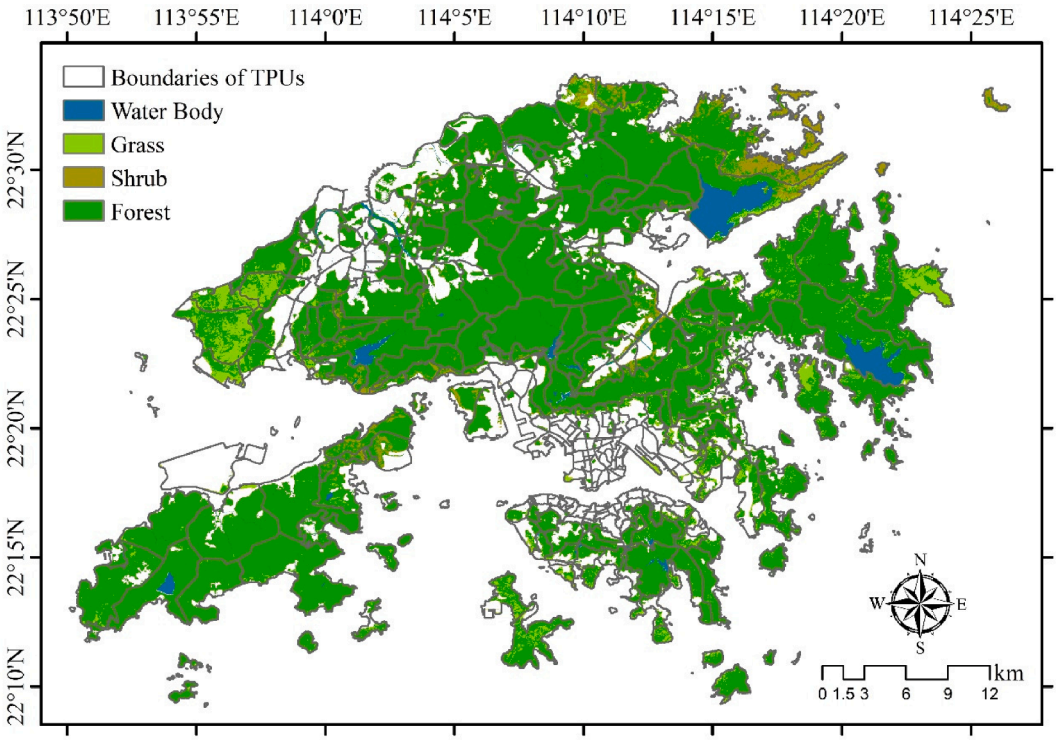

Fig. A3. Map of the total and specific types of greenspace in Hong Kong based on the GlobeLand30 data (30 × 30 m) in 2010.

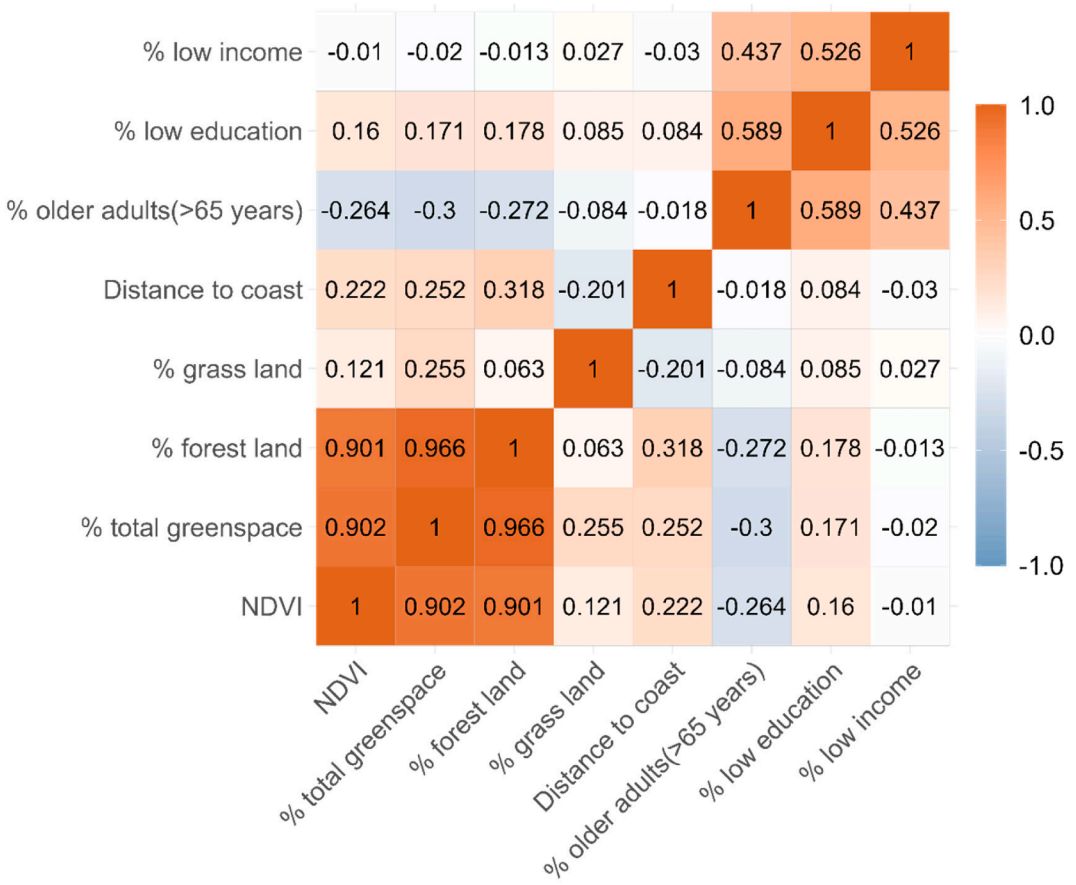

Fig. A4. Spearman's correlation coefficients between area-level indices of greenspace exposure and socio-economic variables, and the variable of blue space exposure.

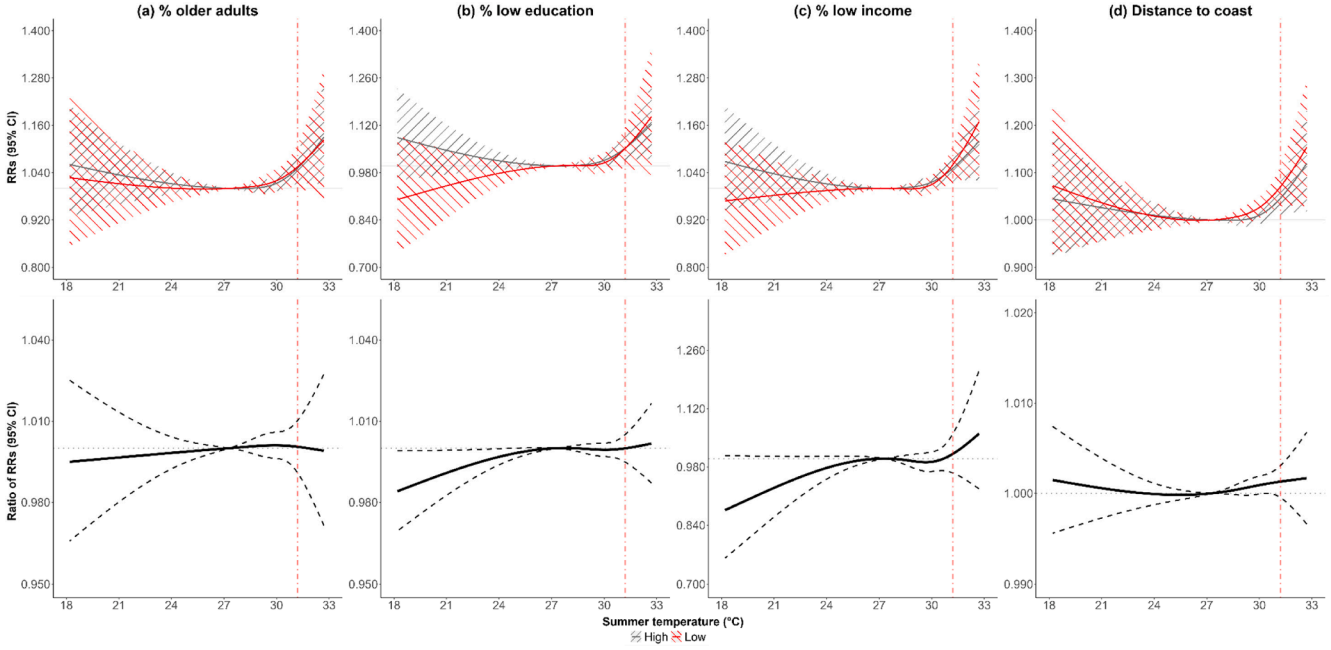

Fig. A5. The relative risks (RRs) (the upper panel) and the ratio of RRs (the lower panel) between the lowest and highest quartiles of each variable of socioeconomic status (SES) and the variable of exposure to water over the whole summer temperature, with 95 % confidence intervals. The SES variables include: a) % older adults (>65 years); b) % low education; c) % low income for each TPU; d) Distance to coast (m). The RRs and the ratio of RRs under extreme heat (at the 99th temperature percentile, 31.2 °C) were indicated in the red dot-dashed line.

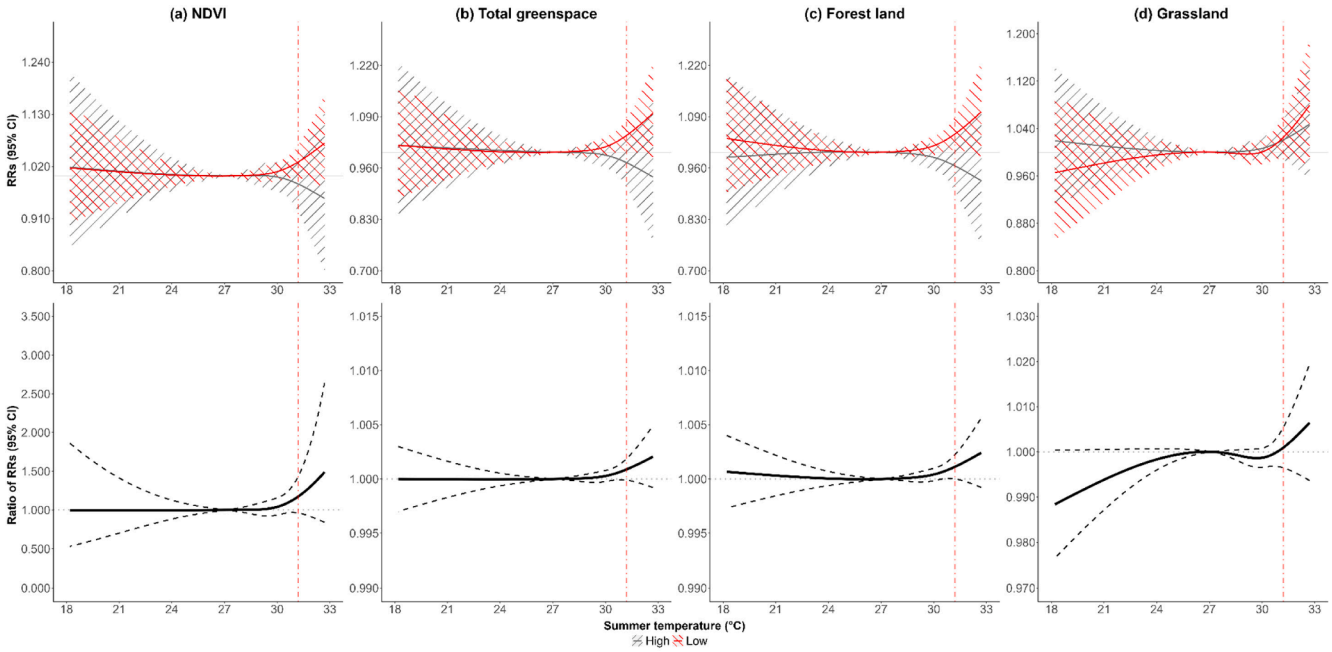

Fig. A6. The relative risks (RRs) (the upper panel) and the ratio of RRs (the lower panel) between the lowest and highest quartiles of each area-level greenspace exposure metric over the whole summer temperature after controlling for the effects of daily relative humidity, O_3 and PM_{10} concentrations at 01 lag days, with 95 % confidence intervals. The area-level greenspace exposure was assessed by the average value of a) NDVI; and the proportion of b) Total greenspace; c) Forest land; d) Grass land for each TPU. The RRs and the ratio of RRs under extreme heat (at the 99th temperature percentile, 31.2 °C) were indicated in the red dot-dashed line.

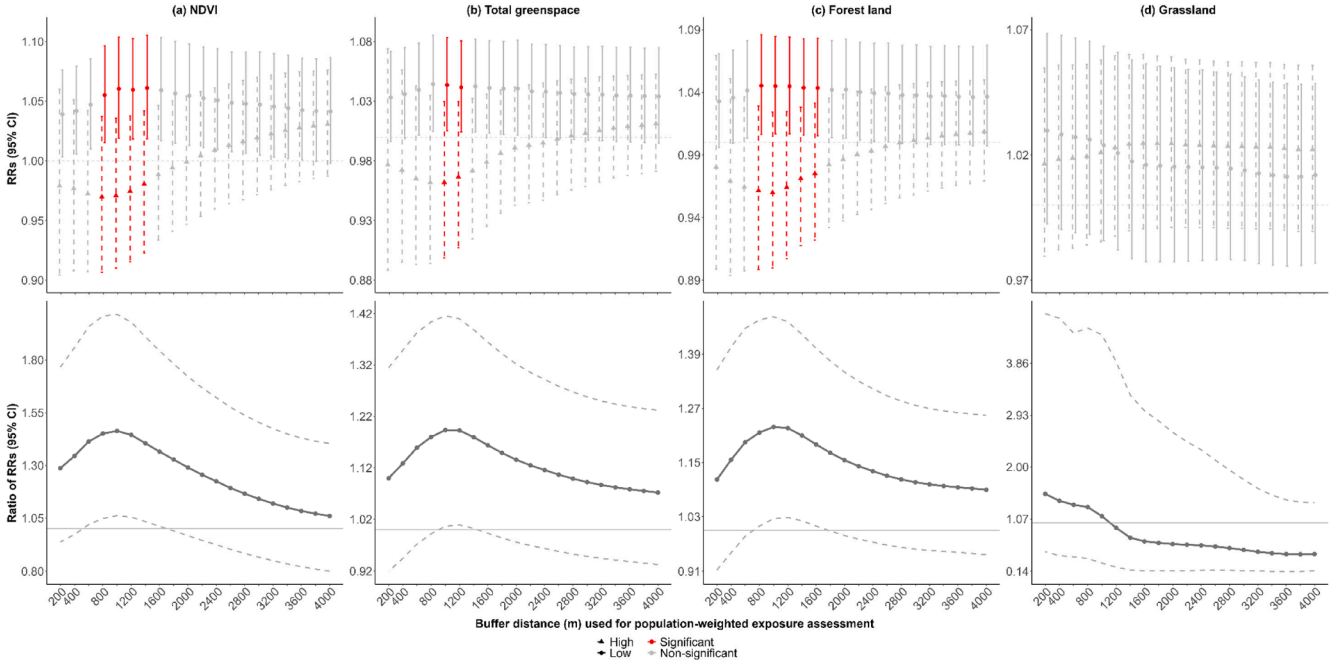

Fig. A7. The relative risks (RRs) and the ratio of RRs between the lowest and highest quartiles of each population-weighted greenspace exposure metric within a buffer distance ranging from 200 m to 4000 m under extreme heat (at the 99th temperature percentile, 31.2 °C) after controlling for the effects of daily relative humidity, O_3 and PM_{10} concentrations at 01 lag days, with 95 % confidence intervals. The greenspace exposure was assessed based on population-weighted metric in terms of: a) NDVI; b) Total greenspace; c) Forest land; d) Grass land.

References

Bian, J., Li, A., Lei, G., Zhang, Z., Nan, X., 2020. Global high-resolution mountain green cover index mapping based on Landsat images and Google Earth Engine. ISPRS J. Photogramm. Remote Sens. 162, 63–76. https://doi.org/10.1016/j.isprsjprs.2020.02.011.

Blanck, H.M., Allen, D., Bashir, Z., Gordon, N., Goodman, A., Merriam, D., Rutt, C., 2012. Let's Go to the Park Today: The Role of Parks in Obesity Prevention and Improving the Public's Health. Child. Obes. 8 (5), 423–428. https://doi.org/10.1089/chi.2012.0085.blan.

Bonan, G.B., 1997. Effects of Land Use on the Climate of the United States. Clim. Change 37 (3), 449–486. https://doi.org/10.1023/A:1005305708775.

Bowler, D.E., Buyung-Ali, L., Knight, T.M., Pullin, A.S., 2010. Urban greening to cool towns and cities: A systematic review of the empirical evidence. Landsc. Urban Plan. 97 (3), 147–155. https://doi.org/10.1016/j.landurbplan.2010.05.006.

Browning, M., Lee, K., 2017. Within What Distance Does "Greenness" Best Predict Physical Health? A Systematic Review of Articles with GIS Buffer Analyses across the

Lifespan. Int. J. Environ. Res. Public Health 14 (7), 675. https://doi.org/10.3390/ijerph14070675.
Browning, M., Rigolon, A., McAnirlin, O., Yoon, H., 2022. Where greenspace matters most: A systematic review of urbanicity, greenspace, and physical health. Landsc. Urban Plan. 217, 104233 https://doi.org/10.1016/j.landurbplan.2021.104233.
Burkart, K., Meier, F., Schneider, A., Breitner, S., Canário, P., Alcoforado, M.J., Scherer, D., Endlicher, W., 2016. Modification of Heat-Related Mortality in an Elderly Urban Population by Vegetation (Urban Green) and Proximity to Water (Urban Blue): Evidence from Lisbon. Portugal. *Environmental Health Perspectives* 124 (7), 927–934. https://doi.org/10.1289/ehp.1409529.
Chen, J., Cao, X., Peng, S., Ren, H., 2017. Analysis and Applications of GlobeLand30: A Review. ISPRS Int. J. Geo Inf. 6 (8), 230. https://doi.org/10.3390/ijgi6080230.
Chen, B., Tu, Y., Wu, S., Song, Y., Jin, Y., Webster, C., Xu, B., Gong, P., 2022a. Beyond green environments: Multi-scale difference in human exposure to greenspace in China. Environ. Int. 166, 107348 https://doi.org/10.1016/j.envint.2022.107348.
Chen, B., Wu, S., Song, Y., Webster, C., Xu, B., Gong, P., 2022b. Contrasting inequality in human exposure to greenspace between cities of Global North and Global South. Nat. Commun. 13 (1), 4636. https://doi.org/10.1038/s41467-022-32258-4.
Choi, H.M., Lee, W., Roye, D., Heo, S., Urban, A., Entezari, A., Vicedo-Cabrera, A.M., Zanobetti, A., Gasparrini, A., Analitis, A., Tobias, A., Armstrong, B., Forsberg, B., Íñiguez, C., Åström, C., Indermitte, E., Lavigne, E., Mayvaneh, F., Acquaotta, F., Bell, M.L., 2022. Effect Modification of Greenness on the Association between Heat and Mortality: A Multi-City Multi-Country Study. eBioMedicine, 84, 104251 https://doi.org/10.1016/j.ebiom.2022.104251.
Ekkel, E.D., De Vries, S., 2017. Nearby green space and human health: Evaluating accessibility metrics. Landsc. Urban Plan. 157, 214–220. https://doi.org/10.1016/j.landurbplan.2016.06.008.
Fouad, A.T.Z., Sinnett, D., Bray, I., McClatchey, R., Reece, R., 2023. Measures of Greenspace Exposure and Their Association to Health-Related Outcomes for the Periods before and during the 2020 Lockdown: A Cross-Sectional Study in the West of England. Land 12 (4), 728. https://doi.org/10.3390/land12040728.
Gasparrini, A., 2022. A tutorial on the case time series design for small-area analysis. BMC Med. Res. Method. 22 (1) https://doi.org/10.1186/s12874-022-01612-x.
Gasparrini, A., Guo, Y., Hashizume, M., Lavigne, E., Zanobetti, A., Schwartz, J., Tobias, A., Tong, S., Rocklöv, J., Forsberg, B., Leone, M., De Sario, M., Bell, M. L., Guo, Y.-L. L., Wu, C., Kan, H., Yi, S.-M., de Sousa Zanotti Stagliorio Coelho, M., Saldiva, P. H. N., … Armstrong, B. (2015). Mortality risk attributable to high and low ambient temperature: A multicountry observational study. *The Lancet*, *386*(9991), 369–375. https://doi.org/10.1016/S0140-6736(14)62114-0.
Gasparrini, A., Guo, Y., Sera, F., Vicedo-Cabrera, A. M., Huber, V., Tong, S., de Sousa Zanotti Stagliorio Coelho, M., Nascimento Saldiva, P. H., Lavigne, E., Matus Correa, P., Valdes Ortega, N., Kan, H., Osorio, S., Kyselý, J., Urban, A., Jaakkola, J. J. K., Ryti, N. R. I., Pascal, M., Goodman, P. G., … Armstrong, B. (2017). Projections of temperature-related excess mortality under climate change scenarios. *The Lancet Planetary Health*, *1*(9), e360–e367. https://doi.org/10.1016/S2542-5196(17)30156-0.
Gasparrini, A., Masselot, P., Scortichini, M., Schneider, R., Mistry, M.N., Sera, F., Macintyre, H.L., Phalkey, R., Vicedo-Cabrera, A.M., 2022. Small-area assessment of temperature-related mortality risks in England and Wales: A case time series analysis. The Lancet Planetary Health 6 (7), e557–e564. https://doi.org/10.1016/S2542-5196(22)00138-3.
Gasparrini, A. (2021). The Case Time Series Design. *Epidemiology (Cambridge, Mass.)*, *32* (6), 829–837. https://doi.org/10.1097/EDE.0000000000001410.
Gronlund, C.J., Zanobetti, A., Wellenius, G.A., Schwartz, J.D., O'Neill, M.S., 2016. Vulnerability to renal, heat and respiratory hospitalizations during extreme heat among U.S. elderly. Clim. Change 136 (3–4), 631–645. https://doi.org/10.1007/s10584-016-1638-9.
Gullón, P., Fontán-Vela, M., Díez, J., Nieuwenhuijsen, M., Rojas-Rueda, D., Escobar, F., Franco, M., 2023. Who benefits from green spaces? Surrounding greenness and incidence of cardiovascular disease in a population-based electronic medical records cohort in Madrid. Int. J. Hyg. Environ. Health 252, 114221. https://doi.org/10.1016/j.ijheh.2023.114221.
Gunawardena, K.R., Wells, M.J., Kershaw, T., 2017. Utilising green and bluespace to mitigate urban heat island intensity. Sci. Total Environ. 584–585, 1040–1055. https://doi.org/10.1016/j.scitotenv.2017.01.158.
Hajna, S., Nafilyan, V., Cummins, S., 2023. Associations between residential greenspace exposure and mortality in 4 645 581 adults living in London, UK: A longitudinal study. The Lancet Planetary Health 7 (6), e459–e468. https://doi.org/10.1016/S2542-5196(23)00057-8.
Harlan, S.L., Declet-Barreto, J.H., Stefanov, W.L., Petitti, D.B., 2013. Neighborhood Effects on Heat Deaths: Social and Environmental Predictors of Vulnerability in Maricopa County. Arizona. *Environmental Health Perspectives* 121 (2), 197–204. https://doi.org/10.1289/ehp.1104625.
Heo, S., Chen, C., Kim, H., Sabath, B., Dominici, F., Warren, J.L., Di, Q., Schwartz, J., Bell, M.L., 2021. Temporal changes in associations between high temperature and hospitalizations by greenspace: Analysis in the Medicare population in 40 U.S. northeast counties. Environ. Int. 156, 106737 https://doi.org/10.1016/j.envint.2021.106737.
Ho, H.C., Fong, K.N.K., Chan, T.-C., Shi, Y., 2020. The associations between social, built and geophysical environment and age-specific dementia mortality among older adults in a high-density Asian city. Int. J. Health Geogr. 19 (1), 53. https://doi.org/10.1186/s12942-020-00252-y.
Holben, B.N., 1986. Characteristics of maximum-value composite images from temporal AVHRR data. Int. J. Remote Sens. 7 (11), 1417–1434. https://doi.org/10.1080/01431168608948945.
Hondula, D.M., Davis, R.E., Georgescu, M., 2018. Clarifying the Connections Between Green Space, Urban Climate, and Heat-Related Mortality. Am. J. Public Health 108 (S2), S62–S63. https://doi.org/10.2105/AJPH.2017.304295.
Hong Kong Census and Statistics Department (HKCSD). (2016). *The 2016 Population By-census*. https://www.censtatd.gov.hk/en/scode459.html.
Hong Kong Environmental Protection Department (HKEPD). (2023). *Environmental Protection Interactive Centre: Air Quality Monitoring Data Searching Paramater*. https://cd.epic.epd.gov.hk/EPICDI/air/station/?lang=en.
Intergovernmental Panel On Climate Change (IPCC), 2023. Climate Change 2022 – Impacts, Adaptation and Vulnerability. In: Working Group II Contribution to the Sixth Assessment Report of the Intergovernmental Panel on Climate Change, (1st ed.). Cambridge University Press. https://doi.org/10.1017/9781009325844.
Iungman, T., Cirach, M., Marando, F., Pereira Barboza, E., Khomenko, S., Masselot, P., Quijal-Zamorano, M., Mueller, N., Gasparrini, A., Urquiza, J., Heris, M., Thondoo, M., Nieuwenhuijsen, M., 2023. Cooling cities through urban green infrastructure: A health impact assessment of European cities. Lancet 401 (10376), 577–589. https://doi.org/10.1016/S0140-6736(22)02585-5.
James, P., Banay, R.F., Hart, J.E., Laden, F., 2015. A Review of the Health Benefits of Greenness. Current Epidemiology Reports 2 (2), 131–142. https://doi.org/10.1007/s40471-015-0043-7.
Kabisch, N., Frantzeskaki, N., Pauleit, S., Naumann, S., Davis, M., Artmann, M., Haase, D., Knapp, S., Korn, H., Stadler, J., Zaunberger, K., Bonn, A., 2016. Nature-based solutions to climate change mitigation and adaptation in urban areas: Perspectives on indicators, knowledge gaps, barriers, and opportunities for action. Ecol. Soc. 21 (2), art39. https://doi.org/10.5751/ES-08373-210239.
Kabisch, N., Van Den Bosch, M., Lafortezza, R., 2017. The health benefits of nature-based solutions to urbanization challenges for children and the elderly – A systematic review. Environ. Res. 159, 362–373. https://doi.org/10.1016/j.envres.2017.08.004.
Kong, F., Yin, H., James, P., Hutyra, L.R., He, H.S., 2014. Effects of spatial pattern of greenspace on urban cooling in a large metropolitan area of eastern China. Landsc. Urban Plan. 128, 35–47. https://doi.org/10.1016/j.landurbplan.2014.04.018.
Kwan, M.-P., 2012. The Uncertain Geographic Context Problem. Ann. Assoc. Am. Geogr. 102 (5), 958–968. https://doi.org/10.1080/00045608.2012.687349.
Lim, C.L., 2020. Fundamental Concepts of Human Thermoregulation and Adaptation to Heat: A Review in the Context of Global Warming. Int. J. Environ. Res. Public Health 17 (21), 7795. https://doi.org/10.3390/ijerph17217795.
Madrigano, J., Mittleman, M.A., Baccarelli, A., Goldberg, R., Melly, S., Von Klot, S., Schwartz, J., 2013. Temperature, Myocardial Infarction, and Mortality: Effect Modification by Individual- and Area-level Characteristics. Epidemiology 24 (3), 439–446. https://doi.org/10.1097/EDE.0b013e3182878397.
Madrigano, J., Ito, K., Johnson, S., Kinney, P.L., Matte, T., 2015. A Case-Only Study of Vulnerability to Heat Wave–RelatedMortality in New York City (2000–2011). Environ. Health Perspect. 123 (7), 672–678. https://doi.org/10.1289/ehp.1408178.
Markevych, I., Schoierer, J., Hartig, T., Chudnovsky, A., Hystad, P., Dzhambov, A.M., De Vries, S., Triguero-Mas, M., Brauer, M., Nieuwenhuijsen, M.J., Lupp, G., Richardson, E.A., Astell-Burt, T., Dimitrova, D., Feng, X., Sadeh, M., Standl, M., Heinrich, J., Fuertes, E., 2017. Exploring pathways linking greenspace to health: Theoretical and methodological guidance. Environ. Res. 158, 301–317. https://doi.org/10.1016/j.envres.2017.06.028.
Masoudi, M., Tan, P.Y., Liew, S.C., 2019. Multi-city comparison of the relationships between spatial pattern and cooling effect of urban green spaces in four major Asian cities. Ecol. Ind. 98, 200–213. https://doi.org/10.1016/j.ecolind.2018.09.058.
Murage, P., Kovats, S., Sarran, C., Taylor, J., McInnes, R., Hajat, S., 2020. What individual and neighbourhood-level factors increase the risk of heat-related mortality? A case-crossover study of over 185,000 deaths in London using high-resolution climate datasets. Environ. Int. 134, 105292 https://doi.org/10.1016/j.envint.2019.105292.
Ng, E., Chen, L., Wang, Y., Yuan, C., 2012. A study on the cooling effects of greening in a high-density city: An experience from Hong Kong. Build. Environ. 47, 256–271. https://doi.org/10.1016/j.buildenv.2011.07.014.
Nieuwenhuijsen, M.J., 2018. Influence of urban and transport planning and the city environment on cardiovascular disease. Nat. Rev. Cardiol. 15 (7), 432–438. https://doi.org/10.1038/s41569-018-0003-2.
Oke, T.R., 1989. The micrometeorology of the urban forest. *Philosophical Transactions of the Royal Society of London. B, Biological.* Sciences 324 (1223), 335–349. https://doi.org/10.1098/rstb.1989.0051.
Panno, A., Carrus, G., Lafortezza, R., Mariani, L., Sanesi, G., 2017. Nature-based solutions to promote human resilience and wellbeing in cities during increasingly hot summers. Environ. Res. 159, 249–256. https://doi.org/10.1016/j.envres.2017.08.016.
Pascal, M., Goria, S., Wagner, V., Sabastia, M., Guillet, A., Cordeau, E., Mauclair, C., Host, S., 2021. Greening is a promising but likely insufficient adaptation strategy to limit the health impacts of extreme heat. Environ. Int. 151, 106441 https://doi.org/10.1016/j.envint.2021.106441.
Pereira Barboza, E., Montana, F., Cirach, M., Iungman, T., Khomenko, S., Gallagher, J., Thondoo, M., Mueller, N., Keune, H., MacIntyre, T., Nieuwenhuijsen, M., 2023. Environmental health impacts and inequalities in green space and air pollution in six medium-sized European cities. Environ. Res. 237, 116891 https://doi.org/10.1016/j.envres.2023.116891.
Qi, X., Wei, L., Laurie, B., Akaki, L., Zhang, X., 2012. Comparison of ArcGIS and SAS Geostatistical Analyst to Estimate Population-Weighted Monthly Temperature for US Counties. Journal of Resources and Ecology 3 (3), 220–229. https://doi.org/10.5814/j.issn.1674-764x.2012.03.004.
Qian, W., Chang, H.H., 2021. Projecting Health Impacts of Future Temperature: A Comparison of Quantile-Mapping Bias-Correction Methods. Int. J. Environ. Res. Public Health 18 (4), 1992. https://doi.org/10.3390/ijerph18041992.

Qin, R., Zhao, Z., Xu, J., Ye, J.-S., Li, F.-M., Zhang, F., 2022. *HRLT: A high-resolution (1 day, 1 km) and long-term (1961–2019) gridded dataset for temperature and precipitation across China* [Preprint]. Meteorology. https://doi.org/10.5194/essd-2022-79.

Qiu, C., Ji, J.S., Bell, M.L., 2021. Effect modification of greenness on temperature-mortality relationship among older adults: A case-crossover study in China. Environ. Res. 197, 111112 https://doi.org/10.1016/j.envres.2021.111112.

Rojas-Rueda, D., Nieuwenhuijsen, M.J., Gascon, M., Perez-Leon, D., Mudu, P., 2019. Green spaces and mortality: A systematic review and meta-analysis of cohort studies. The Lancet Planetary Health 3 (11), e469–e477. https://doi.org/10.1016/S2542-5196(19)30215-3.

Sadeghi, M., Chaston, T., Hanigan, I., De Dear, R., Santamouris, M., Jalaludin, B., Morgan, G.G., 2022. The health benefits of greening strategies to cool urban environments – A heat health impact method. Build. Environ. 207, 108546 https://doi.org/10.1016/j.buildenv.2021.108546.

Schinasi, L.H., Benmarhnia, T., De Roos, A.J., 2018. Modification of the association between high ambient temperature and health by urban microclimate indicators: A systematic review and meta-analysis. Environ. Res. 161, 168–180. https://doi.org/10.1016/j.envres.2017.11.004.

Schindler, M., Le Texier, M., Caruso, G., 2022. How far do people travel to use urban green space? A comparison of three European cities. Appl. Geogr. 141, 102673 https://doi.org/10.1016/j.apgeog.2022.102673.

Sera, F., Armstrong, B., Tobias, A., Vicedo-Cabrera, A. M., Åström, C., Bell, M. L., Chen, B.-Y., de Sousa Zanotti Stagliorio Coelho, M., Matus Correa, P., Cruz, J. C., Dang, T. N., Hurtado-Diaz, M., Do Van, D., Forsberg, B., Guo, Y. L., Guo, Y., Hashizume, M., Honda, Y., Iñiguez, C., … Gasparrini, A. (2019). How urban characteristics affect vulnerability to heat and cold: A multi-country analysis. *International Journal of Epidemiology*, *48*(4), 1101–1112. https://doi.org/10.1093/ije/dyz008.

Son, J.-Y., Lane, K.J., Lee, J.-T., Bell, M.L., 2016. Urban vegetation and heat-related mortality in Seoul, Korea. Environ. Res. 151, 728–733. https://doi.org/10.1016/j.envres.2016.09.001.

Son, J.-Y., Liu, J.C., Bell, M.L., 2019. Temperature-related mortality: A systematic review and investigation of effect modifiers. Environ. Res. Lett. 14 (7), 073004 https://doi.org/10.1088/1748-9326/ab1cdb.

Song, J., Lu, Y., Zhao, Q., Zhang, Y., Yang, X., Chen, Q., Guo, Y., Hu, K., 2022. Effect modifications of green space and blue space on heat–mortality association in Hong Kong, 2008–2017. Sci. Total Environ. 838, 156127 https://doi.org/10.1016/j.scitotenv.2022.156127.

Song, J., Gasparrini, A., Fischer, T., Hu, K., Lu, Y., 2023. Effect Modifications of Overhead-View and Eye-Level Urban Greenery on Heat-Mortality Associations: Small-Area Analyses Using Case Time Series Design and Different Greenery Measurements. Environ. Health Perspect. 131 (9), 097007 https://doi.org/10.1289/EHP12589.

Swanwick, C., Dunnett, N., & Woolley, H. (2003). Nature, Role and Value of Green Space in Towns and Cities: An Overview. *Built Environment (1978-)*, *29*(2), 94–106.

Tatem, A.J., 2017. WorldPop, open data for spatial demography. Sci. Data 4 (1), 170004. https://doi.org/10.1038/sdata.2017.4.

Tucker, C.J., 1979. Red and photographic infrared linear combinations for monitoring vegetation. Remote Sens. Environ. 8 (2), 127–150. https://doi.org/10.1016/0034-4257(79)90013-0.

Wang, R., Helbich, M., Yao, Y., Zhang, J., Liu, P., Yuan, Y., Liu, Y., 2019. Urban greenery and mental wellbeing in adults: Cross-sectional mediation analyses on multiple pathways across different greenery measures. Environ. Res. 176, 108535 https://doi.org/10.1016/j.envres.2019.108535.

Wang, J., Wang, P., Liu, B., Kinney, P.L., Huang, L., Chen, K., 2024. Comprehensive evaluation framework for intervention on health effects of ambient temperature. Eco-Environment & Health 3 (2), 154–164. https://doi.org/10.1016/j.eehl.2024.01.004.

Weier, J., & Herring, D. (2000, August). *Measuring Vegetation (NDVI & EVI)*. NASA Earth Observatory. https://earthobservatory.nasa.gov/features/MeasuringVegetation/measuring_vegetation_1.php.

Wong, K.K., 2009. Urban park visiting habits and leisure activities of residents in Hong Kong. China. *Managing Leisure* 14 (2), 125–140. https://doi.org/10.1080/13606710902752653.

Wu, J., Rappazzo, K.M., Simpson, R.J., Joodi, G., Pursell, I.W., Mounsey, J.P., Cascio, W. E., Jackson, L.E., 2018. Exploring links between greenspace and sudden unexpected death: A spatial analysis. Environ. Int. 113, 114–121. https://doi.org/10.1016/j.envint.2018.01.021.

Xu, Y., Dadvand, P., Barrera-Gómez, J., Sartini, C., Marí-Dell'Olmo, M., Borrell, C., Medina-Ramón, M., Sunyer, J., Basagaña, X., 2013. Differences on the effect of heat waves on mortality by sociodemographic and urban landscape characteristics. J. Epidemiol. Community Health 67 (6), 519–525. https://doi.org/10.1136/jech-2012-201899.

Yang, B.-Y., Zhao, T., Hu, L.-X., Browning, M.H.E.M., Heinrich, J., Dharmage, S.C., Jalaludin, B., Knibbs, L.D., Liu, X.-X., Luo, Y.-N., James, P., Li, S., Huang, W.-Z., Chen, G., Zeng, X.-W., Hu, L.-W., Yu, Y., Dong, G.-H., 2021. Greenspace and human health: An umbrella review. The Innovation 2 (4), 100164. https://doi.org/10.1016/j.xinn.2021.100164.

Yoshikane, T., Yoshimura, K., 2023. A downscaling and bias correction method for climate model ensemble simulations of local-scale hourly precipitation. Sci. Rep. 13 (1), 9412. https://doi.org/10.1038/s41598-023-36489-3.

Zanobetti, A., O'Neill, M.S., Gronlund, C.J., Schwartz, J.D., 2013. Susceptibility to Mortality in Weather Extremes: Effect Modification by Personal and Small-Area Characteristics. Epidemiology 24 (6), 809–819. https://doi.org/10.1097/01.ede.0000434432.06765.91.

Zhang, H., Liu, L., Zeng, Y., Liu, M., Bi, J., Ji, J.S., 2021. Effect of heatwaves and greenness on mortality among Chinese older adults. Environ. Pollut. 290, 118009 https://doi.org/10.1016/j.envpol.2021.118009.

Zhao, Q., Yu, P., Mahendran, R., Huang, W., Gao, Y., Yang, Z., Ye, T., Wen, B., Wu, Y., Li, S., Guo, Y., 2022. Global climate change and human health: Pathways and possible solutions. Eco-Environment & Health 1 (2), 53–62. https://doi.org/10.1016/j.eehl.2022.04.004.

Ziter, C.D., Pedersen, E.J., Kucharik, C.J., Turner, M.G., 2019. Scale-dependent interactions between tree canopy cover and impervious surfaces reduce daytime urban heat during summer. Proc. Natl. Acad. Sci. 116 (15), 7575–7580. https://doi.org/10.1073/pnas.1817561116.